ACSNANO Cite This: ACS Nano XXXX, XXX, XXX–XXX www.acsnano.org

ARTICLE

Fully Packaged Portable Thin Film Biosensor for the Direct Detection of Highly Pathogenic Viruses from On-Site Samples

Jaewon Choi,[†,‡,¶] Minhong Jeun,[†,¶] Seong-Su Yuk,[§,¶] Sungwook Park,[†,‡] Jaebin Choi,[∥] Donggeun Lee,[∥] Hyogeun Shin,[‡,⊥] Hojun Kim,[†] Il-Joo Cho,[‡,⊥] Sang Kyung Kim,[‡,⊥] Seok Lee,[∥] Chang Seon Song,[§] and Kwan Hyi Lee*[,†,‡]

[†]Center for Biomaterials, Korea Institute of Science and Technology (KIST), Seoul 02792, Republic of Korea
[‡]Division of Bio-Medical Science & Technology, KIST School – Korea University of Science and Technology (UST), Seoul 02792, Republic of Korea
[§]Department of Veterinary Medicine, Konkuk University, Seoul 05029, Republic of Korea
[∥]Sensor System Research Center, Korea Institute of Science and Technology (KIST), Seoul 02792, Republic of Korea
[⊥]Center for BioMicrosystems, Korea Institute of Science and Technology (KIST), Seoul 02792, Republic of Korea

Supporting Information

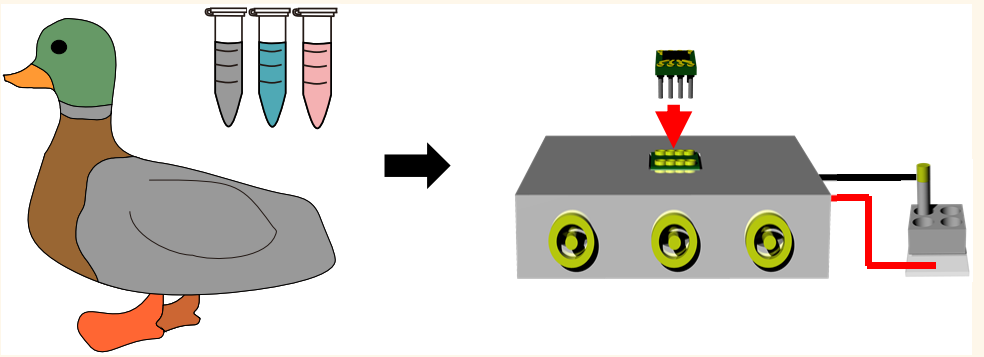

ABSTRACT: **The thin film transistor (TFT) is a promising biosensor system with great sensitivity, label-free detection, and a quick response time. However, even though the TFT sensor has such advantageous characteristics, the disadvantages hamper the TFT sensor's application in the clinical field. The TFT is susceptible to light, noise, vibration, and limited usage, and this significantly limits its on-site potential as a practical biosensor. Herein, we developed a fully packaged, portable TFT electrochemical biosensor into a chip form, providing both portability through minimizing the laboratory equipment size and multiple safe usages by protecting the semiconductor sensor. Additionally, a safe environment that serves as a miniature probe station minimizes the previously mentioned disadvantages, while providing the means to properly link the TFT biosensor with a portable analyzer. The biosensor was taken into a biosafety level 3 (BSL-3) laboratory setting to analyze highly pathogenic avian influenza virus (HPAIV) samples. This virus quickly accumulates within a host, and therefore, early stage detection is critical to deterring the further spread of the deadly disease to other areas. However, current on-site methods have poor limits of detection (10^5–10^6 EID_{50}/mL), and because the virus has low concentration in its early stages, it cannot be detected easily. We have compared the sample measurements from our device with virus concentration data obtained from a RT-PCR (virus range: 10^0–10^4 EID_{50}/mL) and have identified an increasing voltage signal which corresponds to increasing virus concentration.**

KEYWORDS: *chip sensor, rapid detection, avian influenza virus, label-free detection, portable biosensor*

The progress of electrochemical biosensors based on a thin film transistor (TFT) in recent years has been impressive, and electrochemical biosensors are being constantly proposed, with each sensor possessing advanced capabilities compared to its predecessor.[1−10] However, some

Received: October 30, 2018
Accepted: December 21, 2018

DOI: 10.1021/acsnano.8b08298
ACS Nano XXXX, XXX, XXX–XXX

Table 1. AIV Detection Methods between Biosensors[a]

type	target molecule	limit of detection	background solution	sample type	on site	ref
rapid test kit	nucleoprotein	10^5 EID_{50}/mL	lysis buffer	swab sample	O	19
RT-PCR	nucleic acid	10^1 EID_{50}/mL	RT-PCR kit solution	swab sample	X	21
indium−tin-oxide TFT biosensors	nucleoprotein	0.8 pM	0.01× PBS	cultivated cell sample	X	35
silicon nanowire field-effect transistor	antigen	9.6 pM	unknown	synthetic viral surface antigen	X	36
portable TFT sensor	nucleoprotein	10^2 EID_{50}/mL	lysis buffer	swab sample	O	this work

[a]Most biosensors provide either a low LoD or portability but fail to provide both. Additionally, such biosensors have yet to undergo field test to prove they can detect the AIV from real samples.

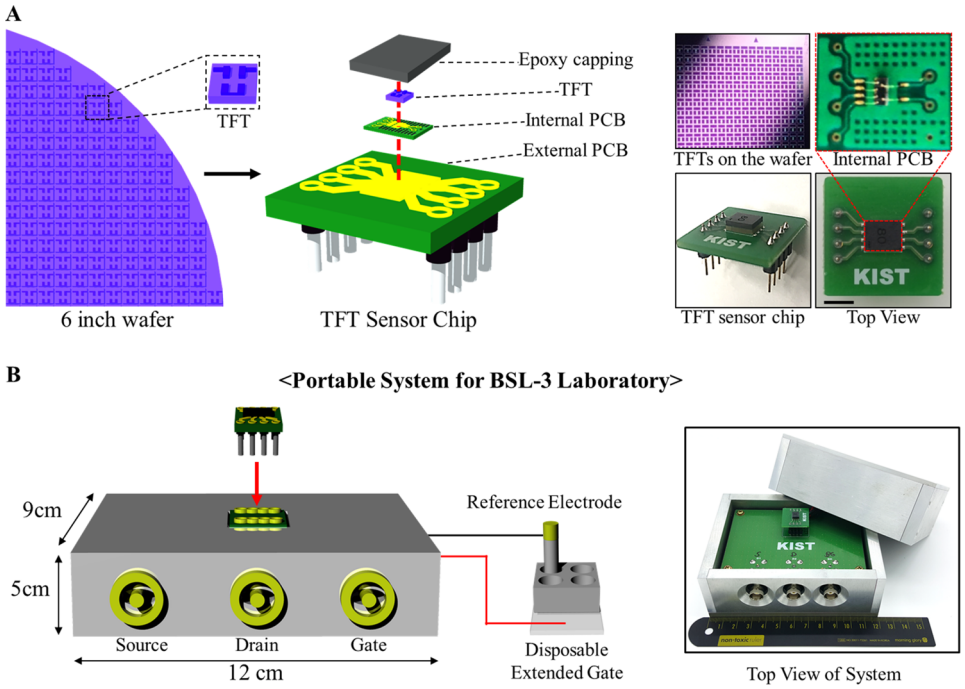

Figure 1. Overall schematic of the packaged biosensor. (A) Packaging and wiring process of the packaged biosensor; the semiconductor portion was extracted from a semiconductor wafer and placed onto a circuited internal PCB layer, where it was subsequently wired using gold wires. The wired semiconductor was then packaged into an external PCB for eventual usage in its respective casing and was sealed with an epoxy layer to prevent degradation of the semiconductor. (B) Minimal pieces required for the packaged biosensor sensor (image is not scaled).

main problems that are characteristic of the electrochemical biosensors have yet to be completely addressed.[11] One such problem is the cumbersome equipment that is characteristic of such biosensors. TFT-based electrochemical biosensors require two portions for detailed analysis: a biochemical interaction/sensing component and a signal detection/analysis component. Generally, depending on the semiconductor utilized, the last portion includes a bulky probe station. Such equipment, although contributing significantly to the biosensors' advantages, cannot be deployed efficiently to analyze on-site field samples. In particular, facilities that host pathogenic viruses, such as highly pathogenic avian influenza viruses (HPAIV), are limited in their utilization of TFT-based electrochemical biosensors.

The recent HPAIV epidemic that originated from China had reached its neighbors in South Korea and Japan.[12,13] The annual migration of water fowl from the Chinese mainland has affected poultry stocks far away as the migratory birds become unwilling and unaware carriers of various variations of the HPAIV.[14,15] Additionally the virus has mutated and has also reached as far as Africa due to the migratory patterns and interaction of migratory birds from different regions.[16] China and South Korea had their respected poultry population decimated, while Europe and Africa also reported record high numbers for infected poultry; for South Korea, the recent 2016 outbreak affected the poultry industry to such an extent that the country had to import eggs from overseas countries. The HPAIV which crossed continents was found to have originated in Asia and became mutated as the migratory birds crossed continents.[17,18] To properly understand the information between the HPAIV and its hosts, the virus was isolated and injected within avian organisms within a biosafety level 3 (BSL-3) laboratory.

A number of different methods have been used to detect the HPAIV (Table 1). Quick on the spot analysis utilizes rapid test kits, which utilize an antibody−antigen reaction mechanism specialized in either cloacal swab samples or mouth swab samples. However, these rapid test kits have a poor limit of detection (LoD) and cannot identify the HPAIV below a certain concentration threshold.[19] Naturally, a detailed sample analysis is undertaken by different methods. The current standard utilizes the reverse transcription polymerase chain reaction (RT-PCR) to amplify the nucleic acid components inside the HPAIV and lower the LoD.[20,21] Other methods

DOI: 10.1021/acsnano.8b08298
ACS Nano XXXX, XXX, XXX−XXX

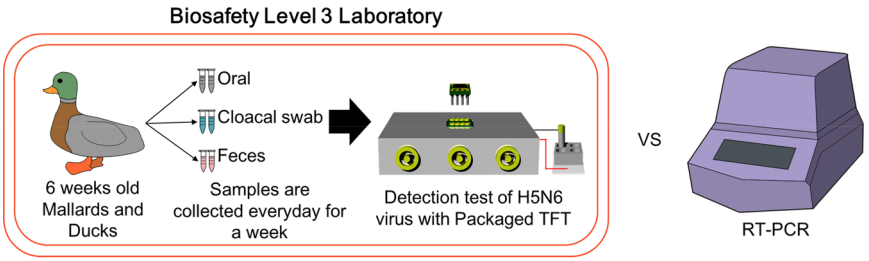

Figure 2. Variety of samples were prepared for measurement within the BSL-3 laboratory. Two main species, mallards and ducks, were grown to 6 weeks of age. They were then injected with the H5N6 avian influenza virus. The virus was incubated within their respective hosts and were collected through oral swabs and cloacal swabs from ducks, oral swab samples from mallards, and feces samples from ducks. The samples were initially analyzed through RT-PCR, and the samples which showed substantial results were selected to be taken and compared by the packaged biosensor.

include using the enzyme-linked immunosorbent assay (ELISA) or isolating the virus.[22,23] However, the methods mentioned above either are subject to low sensitivity or require a time-consuming complex process.

The rapid test kit is subject to poor specificity between 25 and 50%, and a poor LoD of merely $10^{4.5}$−10^{5} EID_{50}/mL.[19,24] The RT-PCR is also not without its own fallacies. As the RT-PCR utilizes sample amplification at its earlier stages, it is subject to error amplification, which only increases as the RT-PCR undergoes more cycles. Indeed, sometimes the RT-PCR itself suffers from reproducibility, and depending on the expertise of the handler, it may cause a cycle difference of up to 10 cycles.[25,26] Additionally, to properly document the presence of an AIV, both oral and cloacal samples should be analyzed together.[27] As a result, methods to properly detect AIV within cloacal samples have garnered interest.

In this work, we have expanded upon the dual gate of the previous sensor and packaged the TFT device into a small and easily transportable state; henceforth, this packaged TFT-based electrochemical biosensor will be identified as a packaged biosensor. This packaged biosensor did not require the heavy analyzing equipment of its predecessors and can be deployed to the site of analysis, which in this case here was a government-certified quarantine institution, such as a BSL-3 laboratory. The basis of the packaged biosensor utilizes the flow of electricity through a transistor which can be affected by charge containing antigen−antibody reactions near the electricity tunnel. The antibodies used for the biosensor are the same antibodies used by the rapid test kit and allow for the direct comparison between those two different platforms. By analyzing the electric current itself, the biosensor is capable of quantitatively assessing the virus amount inside a sample.

The advantages of the packaged biosensor (Figure 1) include the following: (1) the disease or virus in question can be measured without additional chemical deactivation or neutralization; (2) the packaged biosensor is covered and sealed with an epoxy layer, which prevents the degradation of the biosensor device, leading to a longer and more stable lifespan; (3) the packaged biosensor can be deployed to environments unsuitable for large-scale equipment, such as a biosafety level 3 laboratory, or into the field.

The portable biosensor utilizes a modified and tailored metal−oxide semiconductor field-effect transistor (MOSFET) structure. Instead of the traditional MOSFET structure, the biosensor utilizes a dual gate structure and operation, where the thickness of the top gate oxide layer and bottom gate oxide layer are tailored to 14 and 750 nm, respectively, to enhance the sensitivity. The dual gate structure was suggested to utilize the capacitive coupling observed between the top gate oxide and bottom gate oxide in dual gate transistors and consequently to obtain greater sensitivity.

To properly test and use the advantages of the packaged biosensor, the packaged biosensor was deployed to measure the HPAIV H5N6 in a BSL-3 laboratory and was used to analyze a diverse range of samples. This virus is of particular interest due to its evolving characteristics.[28−31] Oral swab samples, cloacal swab samples, and feces samples from 6 week old ducks were analyzed and then compared to RT-PCR measurements (Figure 2). Additionally, to see if the packaged biosensor was capable of sensing the HPAIV from different avian types, mallard oral swab samples were also analyzed.

RESULTS AND DISCUSSION

Validating the Electric Characteristics of the Packaged Biosensor. Before the packaged biosensor can be deployed on site in the near future for data accumulation and analysis, the functionality of the packaged biosensor in the BSL-3 laboratory was tested. Because the TFT biosensor will be comparing the voltage measurement values between a reference measurement and sample measurement, it is imperative to first confirm the stable passage of the current from the source to the drain of the biosensor. Additionally, antigen−antibody reactions upon the reservoirs of the extended gate will influence the flow of the current depending on the amount of antigen within the sample solution and provide sample voltage measurements. Figure 3A describes the drain current *versus* drain voltage experiment, which was initially conducted to test the feasibility of the packaged biosensor. The approximate point of saturation of a drain voltage value of 0.2 V and the drain current increase as the applied voltage increases indicates not only a stable interaction between the SiO_2 gate oxide and the silicon channel layer but also the fact that the biosensor retains its electrical characteristics even after the packaging process.

An additional test for the feasibility and stability of the packaged biosensor was conducted. In Figure 3B, the stability of the packaged biosensor for a prolonged period of time in two different media was analyzed. The phosphate buffered saline (PBS) and lysis buffer from general AIV rapid test kits were chosen for different reasons. PBS is typically used as the standard medium to check the stability and characteristics of a packaged biosensor. The lysis buffer was chosen as it is required in this research as the background medium. The lysis buffer is also required to obtain the nucleoproteins located within the AIV. The time interval of 32 min was chosen because the maximum time required to obtain the biosensor

DOI: 10.1021/acsnano.8b08298
ACS Nano XXXX, XXX, XXX−XXX

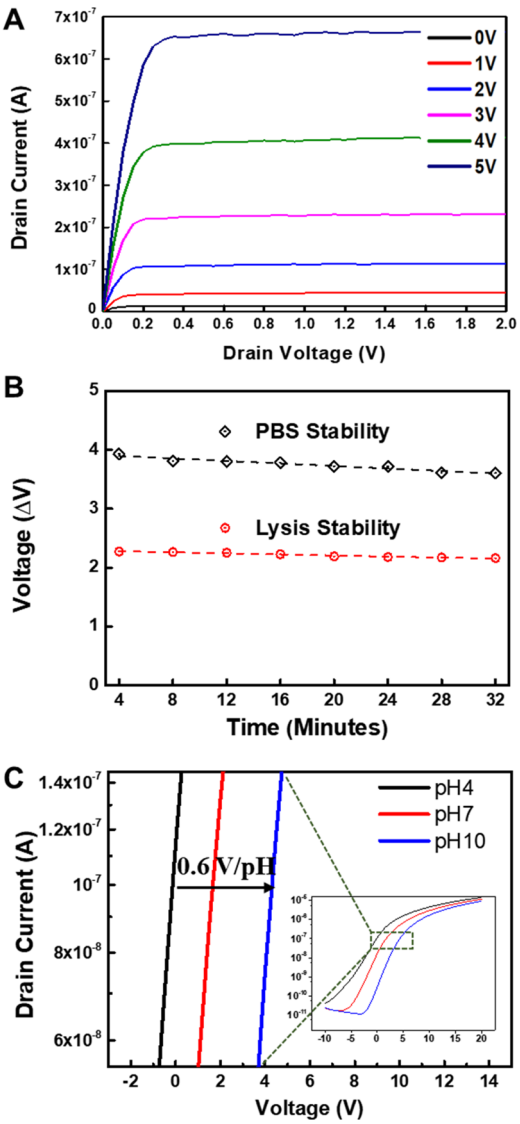

Figure 3. Electric characteristics of the packaged biosensor. (A) Drain current *vs* drain voltage characteristic of the packaged biosensor. (B) Signal stability of different buffer solutions for 32 min. (C) Voltage shift at different pH values.

signal from the AIV sample was 30 min. This 30 min time interval is limited by the 20 min minimum reaction time of the antigen−antibody reaction. This particular time interval of 20 min reflects the time needed for complete saturation of the antibody−antigen reaction (Figure S2). The remaining 10 min includes the signal measurement time and the cleaning procedure, where a gel loading tip was utilized to aspirate the sample and carefully wash the well three times with 100 μL of 1× PBS. For PBS, a slight decrease in the signal was detected as the time progressed. Although the results showed some fluctuation, the fluctuations were miniscule, and especially in the case of the lysis buffer solution, the signal error from the first signal measurement and last signal measurement at 32 min was calculated to be 3.8%.

Figure 3C shows the sensitivity of the packaged biosensor by measuring the change in voltage per the change in pH level. The resulting voltage change per pH was revealed to be 0.6 V/pH, but this value is smaller than that in our previous works, which gave values of 2.0 and 1.8 V/pH, respectively.[3,32] However, the voltage change per pH value of 0.6 V/pH is still well within working parameters as its value is greater than the Nernst limit of 0.06 V/pH[33,34] by a factor of 10. This shows that the packaged biosensor is suitable to be utilized as a highly sensitive sensor.

Nonspecific Binding Test with a Newcastle Virus and No Antibody Coating. To determine the specificity of the antibody, we added the Newcastle virus as it is similar to the HPAIV. The Newcastle virus is generally used to determine the specificity of an AIV antibody. As can be seen in Figure 4A, high Newcastle virus concentrations of 10^5 and 10^6 EID_{50}/mL were added and were allowed to react with the HPAIV-specific antibodies for 20 min. Their effects on the voltage shift were then measured according to the detailed protocol in the Materials and Methods section. The voltage shifts from these two concentrations are 0.010 and 0.011 V.

A second control test was conducted to see whether the antigens influenced the readings by reacting with the sensing gate well surface even without the lack of antibodies. The extended gate was prepared in the same method, but the antibody conjugation step was omitted to produce "antibody-less" extended gates. Then, HPAIV H5N6 concentrations of 10^5 and 10^6 EID_{50}/mL were added to these "antibody-less" reservoirs. After reacting for 20 min, the samples were removed, the well was washed and the sample measured. The small voltage shifts of two H5N6 concentrations indicate that there were no nonspecific binding reactions between the H5N6 antigens and the sensing gate surface. The highest shift value given by a Newcastle virus concentration at 10^6 EID_{50}/mL was designated as the highest noise level for our packaged biosensor. Consequently, as can be seen in Figure 4B, when we conducted a standard experimental test where controlled amounts of HPAIV (from 10^1 to 10^6 EID_{50}/mL) were measured, this noise level of 0.011 V was deemed to be a pseudo threshold for our LoD. Any signal reading below this threshold was deemed to be "unread".

Initial HPAIV Detection from Duck and Mallard Samples. The packaged biosensor was utilized for a diverse array of oral and swab sample measurements. The HPAIV concentration data from the samples were obtained from RT-PCT values and then compared to our packaged biosensor measurements to see if there was any correlation between an increase in concentration from the RT-PCR values and our packaged biosensor voltage shift measurements. Figure 5A shows the recorded packaged biosensor signal compared to the EID_{50}/mL values of random duck oral and cloacal swab samples identified from RT-PCR. When the RT-PCR values corresponded to low EID_{50}/mL concentrations, a fluctuating voltage shift can be observed from the packaged biosensor. The RT-PCR value for such small EID_{50}/mL concentrations was also extrapolated using data from higher concentrations, indicating the value given by the RT-PCR at 10^1 EID_{50}/mL is also tentative at best. Therefore, it is natural for the packaged biosensor to have a hard time analyzing swab samples with such small concentrations. The resulting voltage shift of the three out of five samples is smaller than the threshold voltage of 0.011 V measured, and considering that two samples showed a voltage shift of approximately 0.02 V, the range of the result is large for small concentrations.

Figure 5B shows a positive signal shift of the packaged biosensor as the concentration of the HPAIV in the swab sample increases. The linear fit, when compared to the standard curve line obtained beforehand, has a smaller slope

DOI: 10.1021/acsnano.8b08298
ACS Nano XXXX, XXX, XXX−XXX

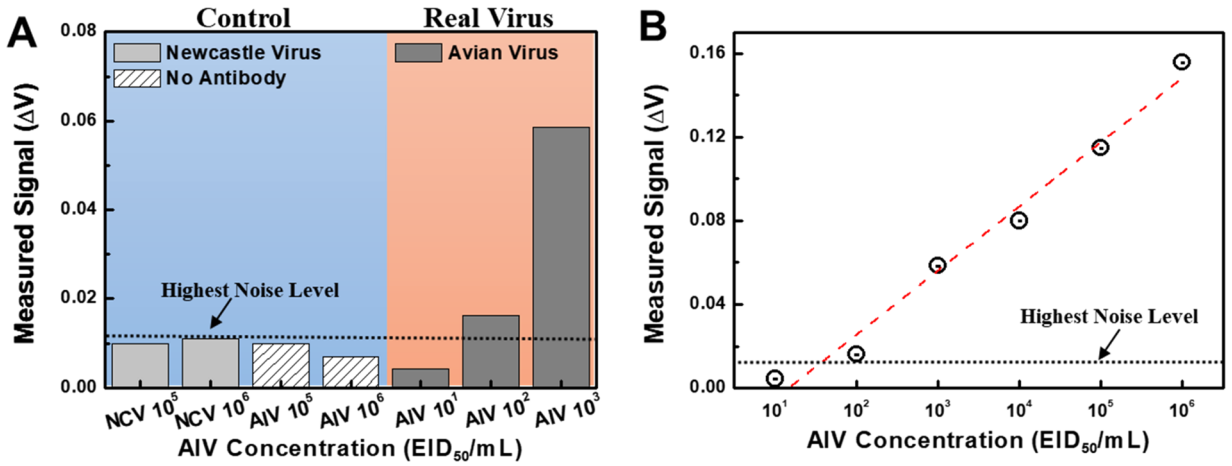

Figure 4. Control experiments for the study. (A) When AIV similar to the Newcastle virus reacts with the HPAIV antibodies and is then washed away, a miniscule shift in voltage can be seen. The striped white boxes indicate a voltage shift recorded when no antibodies were attached to the well surface. (B) Concentration of the HPAIV increases by a factor of 10, and a nearly linear voltage shift increase can be detected. The LoD is 10^2 EID_{50}/mL.

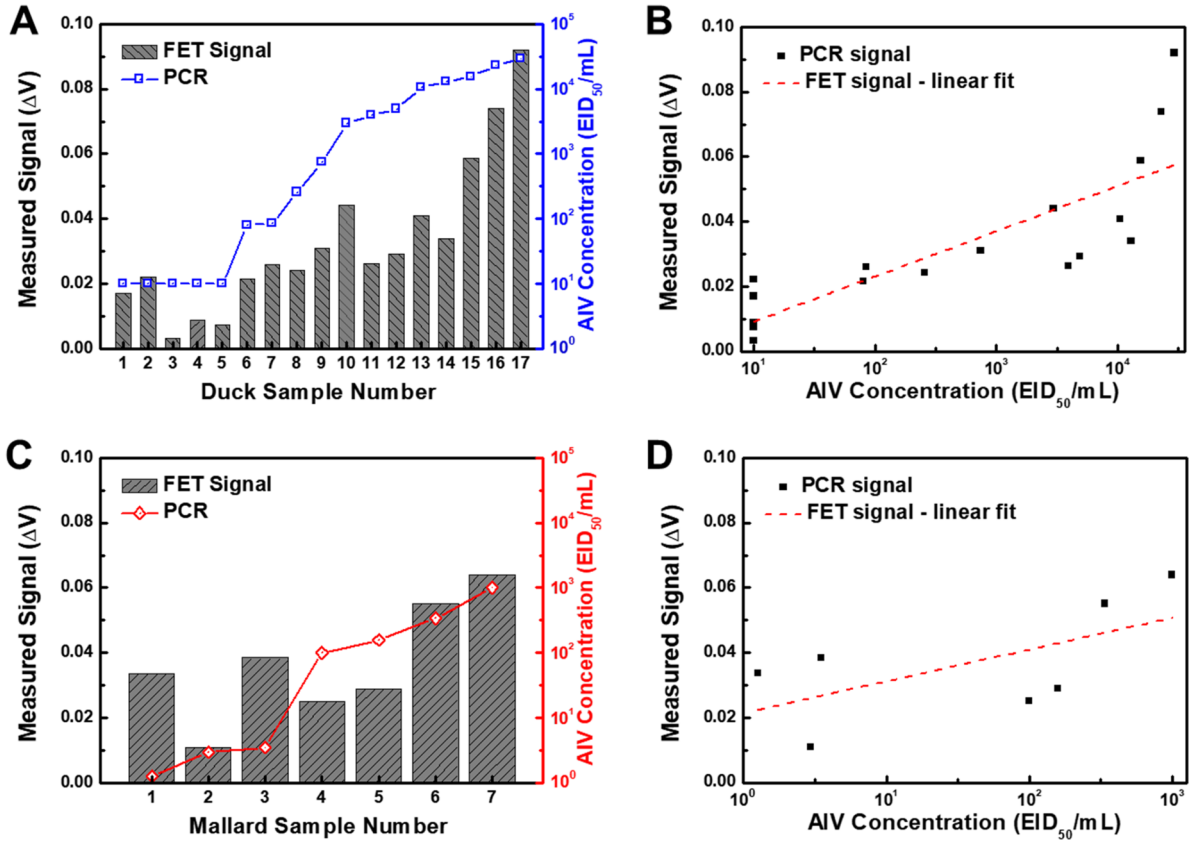

Figure 5. Measured signal values resulting from (A) oral and cloacal swab samples in ducks and (C) oral swab samples in mallards. The columns represent the measured biosensor signals recorded in the swab samples from their respective species. (B,D) Increase of measured signals as the concentration of EID_{50}/mL increases.

and smaller voltage shift values. This is because the samples were real oral swab samples stored in the lysis buffer before measurement, whereas the samples of the standard curve were pure HPAIV viruses suspended in lysis buffer; the physiological conditions of the ducks will affect the reading of the packaged biosensor.

Additionally, in Figure 5C, mallard oral samples were also analyzed. The ability to identify HPAIV within mallard samples is significant. Because the packaged biosensor was designed to be taken with research specific to the field for wildlife avian sample analysis, it was imperative that the packaged biosensor was able to identify HPAIV in samples of mallard origin. Compared to the duck oral samples, the mallard oral samples showed a similar state for low concentration oral samples. A fluctuation was seen in the first three low concentration oral samples. Figure 5D indicates an increase in the voltage shift signal of the packaged biosensor as the concentration of the HPAIV increases. The linear fit shows a more gradual slope

DOI: 10.1021/acsnano.8b08298
ACS Nano XXXX, XXX, XXX−XXX

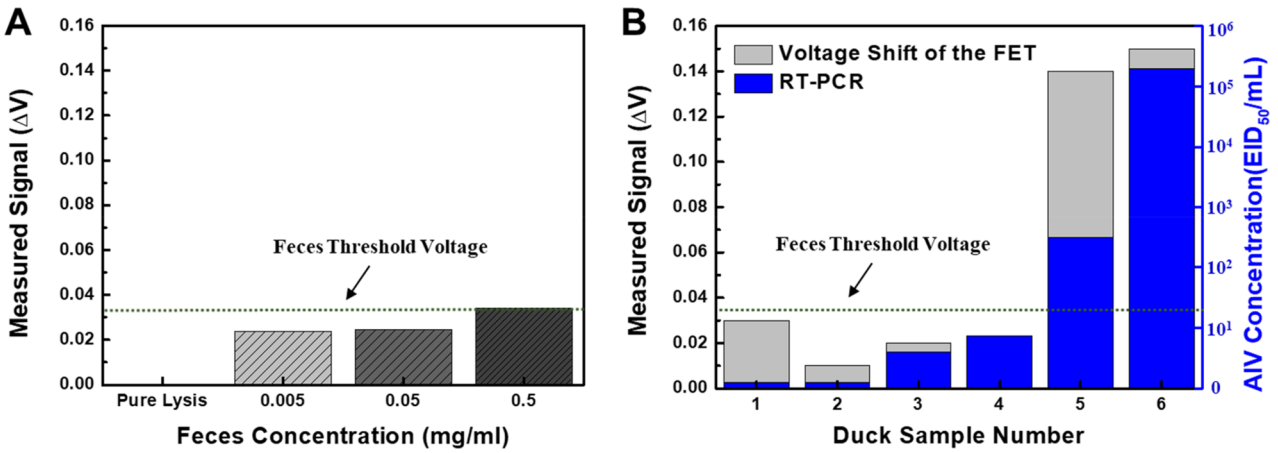

Figure 6. In preparation for real field sample analysis, the biosensor was tested to see if it could properly detect the HPAIV. (A) Measured signals of different feces concentrations on the packaged biosensor shift. (B) Comparison of readings between the packaged biosensor and the RT-PCR.

than that of the duck's version. Because the samples were real oral swab samples from mallards, which exhibit different physiological conditions from the ducks, the results will vary. The characteristics of mallard oral samples influence the packaged biosensor readings at lower concentrations, although that effect eventually lessens as the HPAIV concentration increases.

HPAIV Identification in Raw Feces Samples. To see whether the packaged biosensor was capable of identifying the HPAIV within feces samples, feces samples from HPAIV-injected ducks were acquired and diluted with the lysis buffer to form a 0.5 mg/mL solution. This concentration was determined as it is the concentration of feces samples which are read by the RT-PCR. Before the actual sample could be measured, the effects of a different buffer solution had to be analyzed. Feces samples, although they are diluted in the lysis buffer like oral and cloacal swab samples, ultimately affect the signal from the device due to the solid material floating around within the feces/lysis solution. Therefore, as indicated in Figure 6A, a control test to identify the signal shift from the feces itself was done. Because the background solution is pure lysis buffer, the voltage difference between two pure lysis buffer samples was set to zero. In Figure 6B, all the feces sample measurements were taken by subtracting the voltage shift of the feces/lysis solution from the pure lysis buffer solution. The greatest concentration of 0.5 mg/mL gave a noise value (feces threshold) of 0.032 V.

Overall Comparison between the Biosensor Measurement and RT-PCR Values. Figure 7 indicates the overall HPAIV measurement from injected ducks. The signal from the packaged biosensor was once again compared to the values from the RT-PCR. At low HPAIV concentrations in feces (10^1 EID_{50}/mL), the signal from the packaged biosensor was all below the feces threshold of 0.032 V. However, at higher concentration, the packaged biosensor was able to identify the signal from the feces sample. The ability to detect the feces samples with high concentrations of HPAIV while not detecting the HPAIV at low concentrations indicates that the packaged biosensor functions properly across a specific threshold for feces samples too.

Although the number of mallard oral samples and duck feces samples was small due to the difficulty in proper procurement, a substantial number of oral and cloacal swab samples were

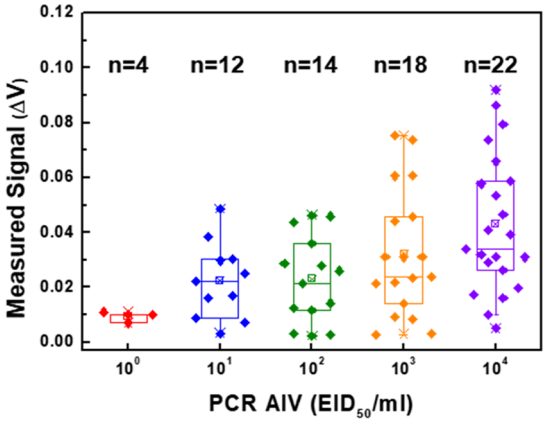

Figure 7. Final 70 swab sample analysis. As the concentration of the HPAIV increases, an increase in the average signal of the packaged biosensor can be seen. Additionally, the range of the packaged biosensor signal also increases as the HPAIV concentration increases. The numbers inside the parentheses indicate the number of samples taken. The top limit and bottom limit of the whiskers indicate 95 and 5%, respectively. The square with the X is the average, and the number within the parentheses indicates the number of samples recorded.

measured for this experiment. A total of 70 samples of either oral or cloacal origin were measured by the packaged biosensor, and the results were compared to the concentration values given by RT-PCR. Once again, as the concentration of the HPAIV within a sample increases, the packaged biosensor signal also showed a corresponding increase.

However, the range of the measurement also increased as the HPAIV concentration increased. Multiple factors explain this phenomenon. First of all, although RT-PCR is the standard for identifying unknown concentrations within a sample, it measures a different object than the packaged biosensor; RT-PCR measures the amount of DNA through amplification. However, the packaged biosensor measures the signal from the sample depending on the concentration of nucleoproteins within the sample. A precise relationship between the amount of DNA and nucleoprotein has yet to be concretely known. Moreover, samples will differ depending on the condition of the duck. A higher HPAIV concentration will lead to more diverse concentrations regarding the

DOI: 10.1021/acsnano.8b08298
ACS Nano XXXX, XXX, XXX−XXX

psychological aspects of the duck specimen. This can be seen in the narrow range and lower concentrations compared to the wider range at higher concentrations. Nevertheless, a positive increase of the packaged biosensor signal corresponding to an increasing concentration of HPAIV is seen.

CONCLUSION

In this study, we have fabricated a fully packaged portable biosensor that is not limited by cumbersome laboratory equipment in its use, and it was utilized in a BSL-3 institute to quantitatively measure HPAIV samples from a number of different sources. Additionally, we have demonstrated its performance using various tests to confirm its possible usage as an on-site detection device that has a multitude of applications in the field. A diverse range of samples with various strains of HPAIV in oral, cloacal, and feces samples which contained a HPAIV strain H5N6 were analyzed within the BSL-3 laboratory. The results from these samples were then compared to the EID_{50}/mL concentrations which were calculated from the CT values provided by RT-PCR tests. Through comparison with the RT-PCR concentration results, we were able to see that our packaged biosensor had a voltage signal which was proportional to the EID_{50}/mL concentrations from the RT-PCR. As the EID_{50}/mL concentrations of the RT-PCR increased in various samples, the packaged biosensor was also able to detect an increasing signal in the same samples. Consequently, the packaged biosensor can be used as a point of care detection device not only for HPAIV but also for other viruses, as well. In an era where point-of-care devices are the target of many researchers due to their potential to serve as field analysts and bedside diagnostic equipment, such a proposition is with great merit.

MATERIALS AND METHODS

Materials. Glutaraldehyde, ethanolamine, and *N*-hydroxysuccinimide, and bovine serum albumin were obtained from Sigma-Aldrich, USA. 1-Ethyl-3-[3-(dimethylamino)propyl]carbodiimide hydrochloride was purchased from Thermo Sciences, USA. The lysis buffer was obtained using the same lysis buffer from the rapid test kit (Bionote: RB2501MH).

HPAIV Sample Preparation. A control experiment was undertaken where the HPAIV strain H5N6 ($10^{8.5}$ EID_{50}/mL) was injected and diluted into pure lysis buffer solution to obtain the wanted concentration (10^{1}–10^{6} EID_{50}/mL). These different concentrations were then measured to observe the effects the concentration had on the packaged biosensor voltage.

Real HPAIV Sample Extraction from Ducks and Mallards. Real swab samples, oral and cloacal, were obtained from 6 week old ducks and mallards which were injected with the H5N6 virus on the first day of the sixth week, as can be seen in the schematic of Figure 2. A total number of 12 ducks and 6 mallards were prepared to serve as hosts for the virus. The swab samples were then added to 200 μL of 1× PBS buffer for storage until further use. To prepare the samples for measurement, 50 μL of the swab sample was mixed with 50 μL of lysis buffer to expose their nucleoproteins for measurement with a packaged biosensor.

The samples chosen to be taken with the packaged biosensor were isolated after obtaining them from the 6 week fowl and processing them with the RT-PCR for initial assessment. The samples with results that were too miniscule for the RT-PCR to detect were discarded as they could not serve as a comparison to the samples results which would be taken by the packaged biosensor. Samples that provided significant values were measured with the packaged biosensor, and the results between the packaged biosensor and RT-PCR were then compared to see whether the packaged biosensor could function properly as planned.

Feces samples from 6 week old ducks injected with the HPAIV were diluted in a lysis buffer solution to a concentration of 0.5 mg of feces per 1 mL of lysis buffer. The same protocol was used to obtain both the 0.05 and 0.005 mg/mL concentrations.

Packaged Biosensor Fabrication. The detailed structure and fabrication procedure of the dual gate TFT device portion was described in our previous work.[19] The packaged biosensor was manufactured as seen in the schematic in Figure 1. A small portion of the silicon on insulator wafer which contained the TFT device was cut and set upon a printed circuit board (PCB). The PCB which is wired directly to the TFT device will be called the internal PCB. The TFT was then wired by gold wires to silver contact pads, which were placed upon the internal PCB. The TFT-wired PCB 1 was then set upon and connected to an external PCB and was covered with an epoxy layer. The wiring for this process also used gold wires and silver contacts. Once the TFT, internal PCB, and external PCB had been properly connected, we termed this complex the packaged biosensor. The silver contact pads on the bottom of the packaged biosensor connect to the packaged biosensor casing, which in turn is connected to our sensing gate, the sensing portion. The packaged biosensor and casing, as can be seen in Figure 1B, are eventually connected to an analyzer, which sends the results to a computer for electrical signal analysis. The casing is connected by triaxial cables to a current–voltage sourcemeter. The casing functions as a miniature probe station and serves to minimalize unwanted noise and minimal light interference.

To manufacture the sensing gate, which contains the surface upon which the antibody antigen reaction takes place, a RF magnetron sputter (50 W, 3 mTorr, 20 sccm argon gas flow) was used to place a 50 nm thick tin dioxide layer on top of an ITO glass. A polydimethylsiloxane (PDMS) reservoir was then attached to this ITO glass through O_2 plasm exposure (5 min). The attached PDMS had wells that had a surface small area of 50 mm^2.

Antibody Fixation to the Bottom Surface of the Sensing Gate. The reservoir area was subject to O_2 (5 min) to provide −OH functional groups to the well bottom of the EG. 3-(Aminopropyl)-triethoxysilane (APTES, 5%) was then inserted into the reservoir for 1 h at room temperature to form $-NH_2$ functional groups on the reservoir bottom. The APTES was removed, and the reservoir was washed with deionized water. Glutaraldehyde was then added, and the reaction occurred at room temperature for 2 h. The glutaraldehyde was removed, and the reservoir was washed with a 20 mmol 2-[4-(2-hydroxyethyl)piperazin-1-yl]ethanesulfonic acid. HPAIV antibodies in PBS were added to the reservoir (0.05 μg/mL) for 1 h at room temperature. The antibodies were removed, and the reservoir was washed with PBS. Ethanolamine (1 M) was added for 1 h, removed, and then washed with PBS. Next, 50 mg/mL bovine serum albumin was added for 1 h, removed, and then washed with PBS.

General Measurement Procedure. The voltage measurement obtained from the TFT biosensor is the difference between a reference curve and a measurement curve. The reference curve is the voltage measurement of the reference solution (blank solution without the target antigen of interest), which in this experiment is the lysis buffer. The reference solution is taken in the antibody-coated reservoir.

After taking the voltage measurement of the reference solution, the blank lysis buffer is taken out and replaced with a virus-containing sample that was prepared in a 1:1 ratio as mentioned above. This virus-containing sample was then allowed to react for 20 min. After 20 min, the sample was taken out and the reservoir was washed with the lysis buffer three times to remove any unbound virus antigen. Then 100 μL of pure lysis buffer was added, and the measurement curve was obtained. The final signal voltage change measurement is the difference between the two obtained curves.

HPAIV Detection Test. The HPAIV strain H5N6 was measured within a BSL-3 environment due to its deadly characteristics. The HPAIV was injected into a lysis buffer (Rapid AIV Ag test kit RG1501MH) solution that had a 1:1 ratio by composition. The HPAIV was allowed to react with the HPAIV antibodies on the bottom surface of the sensing gate for 20 min. This same process

DOI: 10.1021/acsnano.8b08298
ACS Nano XXXX, XXX, XXX–XXX

happened at HPAIV concentrations of 10^2, 10^3, 10^4, 10^5, and 10^6 EID_{50}/mL.

The HPAIV H5N6 was taken within a BSL-3 laboratory due to its harmful nature. Additionally, this provided an environment where the samples were able be measured directly without any prior treatment such as formaldehyde deactivation or contamination during transport. Sample reading for the H5N6 AIV was also taken within the BSL-3 laboratory to simulate an on-site direct analysis environment. This experiment was conducted under a drain voltage of 6 V and a bottom gate sweep voltage ranging from −10 to +20 V.

The reference curves for the two different HPAIV subtypes were obtained by subtracting the antigen-added sample solution from the reference solution. A lysis buffer background solution (100 μL) was initially measured. The background solution was then extracted, and a sample solution with the HPAIV antigen (1:1 ratio) was added into the bottom surface of the sensing gate (100 μL) and then allowed to react with the HPAIV antibody-coated reservoir floor for 20 min. After 20 min, the reservoir was washed with the lysis buffer to wash away the unreacted HPAIV antigens and reinjected with a pure lysis buffer solution (100 μL).

All samples were analyzed with an identical method. An initial background lysis buffer solution that did not possess any HPAIV antigens was added to the well and had its reading recorded. This reference solution was then taken out, and the well had the sample added to the well. After 20 min, the sample solution was washed with PBS to wash away antigen molecules that did not bind to the antibodies, and a reference solution was added once again to analyze voltage change that was a result of only the captured antigens.

ASSOCIATED CONTENT

Supporting Information

The Supporting Information is available free of charge on the ACS Publications website at DOI: 10.1021/acsnano.8b08298.

Rapid test kit detection, antibody−antigen reaction saturation point identification, RT-PCR concentration measurements from cloacal and oral swab samples (PDF)

AUTHOR INFORMATION

Corresponding Author

*Phone: +82-2-958-6804. Fax: +82-2-958-5308. E-mail: kwanhyi@kist.re.kr.

ORCID

Kwan Hyi Lee: 0000-0002-7891-844X

Author Contributions

¶J.C., M.J., and S.-S.Y. contributed equally to this work.

Notes

The authors declare no competing financial interest.

ACKNOWLEDGMENTS

This study was supported by the Bio & Medical Technology Development Program of the NRF funded by the Korean government MSIP (2015M3A9E2029265), and R&D Convergence Program of National Research Council of Science & Technology (NST) of Republic of Korea (CAP-16-02-KIST).

REFERENCES

(1) Choi, J.; Seong, T. W.; Jeun, M.; Lee, K. H. Field-Effect Biosensors for On-Site Detection: Recent Advances and Promising Targets. *Adv. Healthcare Mater.* **2017**, *6*, 1700796.

(2) Kang, B. J.; Jeun, M.; Jang, G. H.; Song, S. H.; Jeong, I. G.; Kim, C.-S.; Searson, P. C.; Lee, K. H. Diagnosis of Prostate Cancer *via* Nanotechnological Approach. *Int. J. Nanomed.* **2015**, *10*, 6555−6569.

(3) Seong, T. W.; Seo, J. M.; Lee, K. H. Full Length Histone H3 Conjugated Electrochemical Biosensor for Extracellular Proteolytic Cathepsin L Activity. *Sens. Actuators, B* **2018**, *267*, 237−244.

(4) Abdulbari, H. A.; Basheer, E. A. M. Electrochemical Biosensors: Electrode Development, Materials, Design, and Fabrication. *ChemBioEng Rev.* **2017**, *4*, 92−105.

(5) Zhu, C.; Yang, G.; Li, H.; Du, D.; Lin, Y. Electrochemical Sensors and Biosensors Based on Nanomaterials and Nanostructures. *Anal. Chem.* **2015**, *87*, 230−249.

(6) Min, J.; Nothing, M.; Coble, B.; Zheng, H.; Park, J.; Im, H.; Weber, G. F.; Castro, C. M.; Swirski, F. K.; Weissleder, R.; Lee, H. Integrated Biosensor for Rapid and Point-Of-Care Sepsis Diagnosis. *ACS Nano* **2018**, *12*, 3378−3384.

(7) Ganguli, A.; Watanabe, Y.; Hwang, M. T.; Huang, J.-C.; Bashir, R. Robust Label-Free MicroRNA Detection Using One Million ISFET Array. *Biomed. Microdevices* **2018**, *20*, 45.

(8) Kim, J.; Stockton, A. M.; Jensen, E. C.; Mathies, R. A. Pneumatically Actuated Microvalve Circuits for Programmable Automation of Chemical and Biochemical Analysis. *Lab Chip* **2016**, *16*, 812−819.

(9) Choi, D.-H.; Li, Y.; Cutting, G. R.; Searson, P. C. A Wearable Potentiometric Sensor with Integrated Salt Bridge for Sweat Chloride Measurement. *Sens. Actuators, B* **2017**, *250*, 673−678.

(10) Lum, J.; Wang, R.; Hargis, B.; Tung, S.; Bottje, W.; Lu, H.; Li, Y. An Impedance Aptasensor with Microfluidic Chips for Specific Detection of H5N1 Avian Influenza Virus. *Sensors* **2015**, *15*, 18565−18578.

(11) Grieshaber, D.; MacKenzie, R.; Vörös, J.; Reimhult, E. Electrochemical Biosensors - Sensor Principles and Architectures. *Sensors* **2008**, *8*, 1400−1458.

(12) Kim, H. K.; Jeong, D. G.; Yoon, S.-W. Recent Outbreaks of Highly Pathogenic Avian Influenza Viruses in South Korea. *Clin. Exp. Vaccine Res.* **2017**, *6*, 95−103.

(13) Okamatsu, M.; Ozawa, M.; Soda, K.; Takakuwa, H.; Haga, A.; Hiono, T.; Matsuu, A.; Uchida, Y.; Iwata, R.; Matsuno, K.; Kuwahara, M.; Yabuta, T.; Usui, T.; Ito, H.; Onuma, M.; Sakoda, Y.; Saito, T.; Otsuki, K.; Ito, T.; Kida, H. Characterization of Highly Pathogenic Avian Influenza Virus A(H5N6), Japan, November 2016. *Emerging Infect. Dis.* **2017**, *23*, 691−695.

(14) Kim, H.-R.; Lee, Y.-J.; Park, C.-K.; Oem, J.-K.; Lee, O.-S.; Kang, H.-M.; Choi, J.-G.; Bae, Y.-C. Highly Pathogenic Avian Influenza (H5N1) Outbreaks in Wild Birds and Poultry, South Korea. *Emerging Infect. Dis.* **2012**, *18*, 480−483.

(15) Kwon, J.-H.; Lee, D.-H.; Swayne, D. E.; Noh, J.-Y.; Yuk, S.-S.; Erdene-Ochir, T.-O.; Hong, W.-T.; Jeong, J.-H.; Jeong, S.; Gwon, G.-B.; Lee, S.; Song, C.-S. Reassortant Clade 2.3.4.4 Avian Influenza A(H5N6) Virus in a Wild Mandarin Duck, South Korea, 2016. *Emerging Infect. Dis.* **2017**, *23*, 822−826.

(16) Lee, D.-H.; Bertran, K.; Kwon, J.-H.; Swayne, D. E. Evolution, Global Spread, and Pathogenicity of Highly Pathogenic Avian Influenza H5Nx Clade 2.3.4.4. *J. Vet. Sci.* **2017**, *18*, 269−280.

(17) Winker, K.; Gibson, D. D. The Asia-to-America Influx of Avian Influenza Wild Bird Hosts Is Large. *Avian Dis.* **2010**, *54*, 477−482.

(18) Meseko, C. A.; Oladokun, A. T.; Ekong, P. S.; Fasina, F. O.; Shittu, I. A.; Sulaiman, L. K.; Egbuji, A. N.; Solomon, P.; Ularamu, H. G.; Joannis, T. M. Rapid Antigen Detection in the Diagnosis of Highly Pathogenic Avian Influenza (H5N1) Virus in Nigeria. *Diagn. Microbiol. Infect. Dis.* **2010**, *68*, 163−165.

(19) Park, S.; Choi, J.; Jeun, M.; Kim, Y.; Yuk, S.-S.; Kim, S. K.; Song, C.-S.; Lee, S.; Lee, K. H. Detection of Avian Influenza Virus from Cloacal Swabs Using a Disposable Well Gate FET Sensor. *Adv. Healthcare Mater.* **2017**, *6*, 1700371.

(20) de Jong, M. D.; Hien, T. T. Avian Influenza A (H5N1). *J. Clin. Virol.* **2006**, *35*, 2−13.

(21) Chen, W.; He, Bo.; Li, C.; Zhang, X.; Wu, W.; Yin, X.; Fan, B.; Fan, X.; Wang, J. Real-Time RT-PCR for H5N1 Avian Influenza A Virus Detection. *J. Med. Microbiol.* **2007**, *56*, 603−607.

(22) He, Q.; Velumani, S.; Du, Q.; Lim, C. W.; Ng, F. K.; Donis, R.; Kwang, J. Detection of H5 Avian Influenza Viruses by Antigen-

DOI: 10.1021/acsnano.8b08298
ACS Nano XXXX, XXX, XXX−XXX

capture Enzyme-Linked Immunosorbent Assay Using H5-Specific Monoclonal Antibody. *Clin. Vaccine Immunol.* **2007**, *14*, 617−623.
(23) Wang, R.; Taubenberger, J. K. Methods for Molecular Surveillance of Influenza. *Expert Rev. Anti-Infect. Ther.* **2010**, *8*, 517−527.
(24) Wibowo, M. H.; Untari, T.; Artanto, S.; Putri, K.; Amanu, S.; Asmara, W. Evaluation of Rapid Detection Kit Against Avian Influenza A Virus and H5 Subtype for Field Sample. *Indones. J. Biotechnol.* **2017**, *21*, 48−55.
(25) Bustin, S. A. Absolute Quantification of mRNA Using Real-time Reverse Transcription Polymerase Chain Reaction Assays. *J. Mol. Endocrinol.* **2000**, *25*, 169.
(26) Bustin, S. A. Quantification of mRNA Using Real-Time Reverse Transcription PCR (RT-PCR): Trends and Problems. *J. Mol. Endocrinol.* **2002**, *29*, 23−39.
(27) Jindal, N.; de Abin, M.; Primus, A. E.; Raju, S.; Chander, Y.; Redig, P. T.; Goyal, S. M. Comparison of Cloacal and Oropharyngeal Samples for the Detection of Avian Influenza Virus in Wild Birds. *Avian Dis.* **2010**, *54*, 115−119.
(28) Mok, C. K. P.; Da Guan, W.; Liu, X. Q.; Lamers, M. M.; Li, X. B.; Wang, M.; Zhang, T. J. S.; Zhang, Q. L.; Li, Z. T.; Huang, J. C.; Lin, J. Y.; Zhang, Y. H.; Zhao, P.; Lee, H. H. Y.; Chen, L.; Li, Y. M.; Peiris, J. S. M.; Chen, R. C.; Zhong, N. S.; Yang, Z. F. Genetic Characterization of Highly Pathogenic Avian Influenza A(H5N6) Virus, Guangdong, China. *Emerging Infect. Dis.* **2015**, *21*, 2268−2271.
(29) Si, Y.-J.; Lee, I. W.; Kim, E.-H.; Kim, Y.-I.; Kwon, H.-I.; Park, S.-J.; Nguyen, H. D.; Kim, S. M.; Kwon, J.-J.; Choi, W.-S.; Beak, Y. H.; Song, M.-S.; Kim, C.-J.; Webby, R. J.; Choi, Y.-K. Genetic Characterisation of Novel, Highly Pathogenic Avian Influenza (HPAI) H5N6 Viruses Isolated in Birds, South Korea, November 2016. *Euro. Surveill.* **2017**, *22*, 30434.
(30) Sun, H.; Pu, J.; Wei, Y.; Sun, Y.; Hu, J.; Liu, L.; Xu, G.; Gao, W.; Li, C.; Zhang, X.; Huang, Y.; Chang, K.-C.; Liu, X.; Liu, J. Highly Pathogenic Avian Influenza H5N6 Viruses Exhibit Enhanced Affinity for Human Type Sialic Acid Receptor and In-Contact Transmission in Model Ferrets. *J. Virol.* **2016**, *90*, 6235−6243.
(31) Li, M.; Zhao, N.; Luo, J.; Li, Y.; Chen, L.; Ma, J.; Zhao, L.; Yuan, G.; Wang, C.; Wang, Y.; Liu, Y.; He, H. Genetic Characterization of Continually Evolving Highly Pathogenic H5N6 Influenza Viruses in China, 2012−2016. *Front. Microbiol.* **2017**, *8*, 260.
(32) Jeun, M.; Park, S.; Kim, Y.; Choi, J.; Song, S. H.; Jeong, I. G.; Kim, C.-S.; Lee, K. H. Self-Normalized Detection of ANXA3 from Untreated Urine of Prostate Cancer Patients without Digital Rectal Examination. *Adv. Healthcare Mater.* **2017**, *6*, 1700449.
(33) Go, J.; Nair, P. R.; Reddy, B.; Dorvel, B.; Bashir, R.; Alam, M. A. Beating the Nernst Limit of 59mV/pH with Double-Gated Nano-Scale Field-Effect Transistors and Its Applications to Ultra-Sensitive DNA Biosensors. *2010 International Electron Devices Meeting*, San Francisco, CA, Dec 8−10, 2010; 8.7.1−8.7.4.
(34) Knopfmacher, O.; Tarasov, A.; Fu, W.; Wipf, M.; Niesen, B.; Calame, M.; Schönenberger, C. Nernst Limit in Dual-Gated Si-Nanowire FET Sensors. *Nano Lett.* **2010**, *10*, 2268−2274.
(35) Guo, D.; Zhuo, M.; Zhang, X.; Xu, C.; Jiang, J.; Gao, F.; Wan, Q.; Li, Q.; Wang, T. Indium-Tin-Oxide Thin Film Transistor Biosensors for Label-Free Detection of Avian Influenza virus H5N1. *Anal. Chim. Acta* **2013**, *773*, 83−88.
(36) Kim, J.-Y.; Ahn, J.-H.; Moon, D.-I.; Park, T. J.; Lee, S. Y.; Choi, Y. K. Multiplex Electrical Detection of Avian Influenza and Human Immunodeficiency Virus with an Underlap-Embedded Silicon Nanowire Field-Effect Transistor. *Biosens. Bioelectron.* **2014**, *55*, 162−167.

DOI: 10.1021/acsnano.8b08298
ACS Nano XXXX, XXX, XXX−XXX